Spatial adaptivity in SOLEDGE3X-HDG for edge plasma simulations in versatile magnetic and reactor geometries

Giacomo Piraccini, Frédéric Schwander, Eric Serre, Giorgio Giorgiani, Manuel Scotto D'abusco

Spatial adaptivity in SOLEDGE3X-HDG for edge plasma simulations in versatile magnetic and reactor geometries

G. Piraccini*, F. Schwander, E. Serre, G. Giorgiani, M. Scotto D'Abusco

June 23, 2023

Aix Marseille Univ, CNRS, Centrale Marseille, M2P2, Marseille, France

Abstract

With the ultimate goal to predict plasmas heat and particle fluxes in ITER operation, more efforts are required to deal with realistic magnetic configurations and tokamak geometries. In an attempt to achieve this goal, we propose an adaptive mesh refinement method added to a fluid solver based on a high-order hybrid discontinuous Galerkin (HDG) method. Based on unstructured meshes, this magnetic equilibrium free numerical scheme has shown promising and encouraging features to solve 2D/3D transport reduced Braginski fluid equations. To improve its numerical efficiency, a mesh refinement based on h-adpativity is investigated. We describe here an adaptive refinement strategy on a reduced edge particle transport model based on electron density and parallel momentum. This strategy is illustrated in realistic tokamak wall geometry. Computations performed show potential gains in the required number of degrees of freedom against benchmark computations with uniform meshes, along with the potential to give an automated, goal-oriented, mesh generation technique for edge transport simulations in 2D.

Spatial adaptivity; hybrid discontinuous galerkin; fusion; plasma physics; h-refinement

1 Introduction

The control of heat fluxes onto the tokamak walls in high energy confinement configurations, for both steady-state and transient regimes must be addressed to successfully run future ITER experiments. Sustaining burning plasmas in the core of the machine while achieving sufficient power spreading on the dedicated wall components to keep the heat flux below the handling capability of the materials imposes stringent, and conflicting constraints on

the tokamak operation. This leads to the design of experiments in ITER being able to remove the bulk of the energy before it contacts the wall components. The difficulty to get global experimental measurements in tokamak, particularly with a nuclear environment in ITER, makes complementary numerical simulations a valuable asset in interpreting experiments and adjust the magnetic configuration and plasma parameters to the edge plasma conditions. Thus, reliable numerical simulations are required in realistic tokamak conditions to better understand how turbulence and transport drive the heat and the particle from the core to the wall. However, the capability of current solvers to perform such simulations is still acknowledged by the international community as being largely insufficient. A strong scale-up of these simulations is required for successful applications to a tokamak of unprecedented size. In this framework, we have identified that high-order finite-element methods have the potential to satisfy this objective to progress towards predictive plasma simulations of ITER. More precisely, we have implemented a Hybrid Discontinuous Galerkin (HDG) method to solve 2D/3D transport equations for a fluid Braginskii model in the whole vacuum chamber whatever the geometrical complexity, and eventually for non-steady magnetic equilibrium [1], a critical point to model the discharge start-up phase. Due to the capability of the solver we are able to handle structured, unstructured and overall non-aligned meshes with the magnetic field. To improve the efficiency of this solver and target ITER simulations, we present in this work an adaptive mesh refinement method to dynamically re-adjust the mesh within certain sensitive regions and locally decrease the error. This new feature leads to an increase of accuracy of the solution and allows first solving problems with coarse meshes, that are then refined to capture large local gradients usually found between edge and scrape-off layer (SOL), following specific error estimators of the output. These error estimators result in a spatial error distribution, which is then used to drive the adaptive refinement strategy, leading to a local mesh subdivision, that is the h-refinement. This allows to consider the whole domain with edge and core with a mesh adaptively refined in the areas of greater interest, such as the separatrix (or Last Closed Flux Surface in limited plasmas) and the SOL while the parts that do not require fine resolution of the solution are coarsened. The realization of the adaptive part is made with Mmg, an open source software for simplicial remeshing [2, 3], that is linked to the HDG main code. In this paper, we would like to show the possibility to adapt the mesh iteratively on a reduced 2D model for ion density n and particle flux Γ in the direction parallel to the magnetic field, by following several error estimators strategies in order to demonstrate the usefulness of an adaptive method. This simplified 2D model involves the basic physical aspects that are required in the 3D transport analysis, combined with a complete set of numerical tasks already findable in more complex models. A particular effort is put into the identification of relevant error estimators that can accommodate the fact that plasma properties, and

therefore absolute errors, vary by several orders of magnitude between the core and the wall. These estimators are then exploited to devise refinement strategies that can adequately refine the mesh where required, typically in the neighborhood of the separatrix and close to the wall, while reducing the memory and computational cost of the simulation.

2 Physical Model

The standard way to investigate turbulence and transport in the plasma edge under high-collisionality conditions [4], is a fluid model based on Braginskii equations, associated with Bohm boundary conditions at the plasmaâĂŞwall interface. We have considered both a circular geometry with limiter and realistic WEST tokamak geometry, both restricted to the edge and SOL regions. The strong intensity of the magnetic field $\mathbf{B}$ leads to a specific flow direction, along which the governing equations are projected using differential operators: $\nabla_{\parallel} = \mathbf{b} \cdot \nabla$ and $\nabla_{\perp} = \nabla - \mathbf{b}\nabla_{\parallel}$, where $\mathbf{b} = \frac{\mathbf{B}}{\|\mathbf{B}\|}$ is the unitary vector parallel to the magnetic field. Using simplified closures developed by Braginskii, the two-dimensional fluid conservation equations for electrons and ions can be derived. Under some hypotheses and ordering [4], a minimum system involving the ion density n and parallel momentum $\Gamma = nu$ can be considered. Then, considering the quasi-neutral limit ($n_e \approx Zn_i$) and neglecting the electron inertia ($\frac{m_e}{m_i} \simeq O(10^{-3})$), the system for an isothermal plasma is:

$$\partial_t n + \nabla \cdot (nu\boldsymbol{b}) - \nabla \cdot (D\nabla_{\perp} n) = S_n \tag{1}$$

$$\partial_t (nu) + \nabla \cdot (nu^2\boldsymbol{b}) + \nabla_{\parallel}(c_s^2 n) - \nabla \cdot (\mu\nabla_{\perp} nu) = S_{\Gamma} \tag{2}$$

The variable c_s refers to the speed of sound while S_n and S_{Γ} are the sources that drive the particle and momentum flux, respectively. The effective diffusion coefficients D and μ are taken into account for both collisional transport and turbulence in the cross-field direction (described via a gradient diffusion hypothesis). They are assumed to be uniform in the poloidal cross-section. In this paper, they are also assumed to be equal, $D = \mu$. The non-dimensionalization used to obtain this system can be found in the reference [4]. The system under considerations is dissipative and yields no instabilities and we have therefore considered the steady-state version of the model presented for the whole set of simulations carried out and showed in this paper.

2.1 Boundary conditions

The system is provided with appropriate boundary conditions modelling the plasmaâĂŞwall interaction: at the wall, the density is left free, and the plasmaâĂŞwall interaction is usually described by the Bohm boundary condition

for the parallel velocity [4]. This imposes an outgoing sonic isothermal velocity at the wall, such that:

$$\frac{u}{c_s} = M = \pm 1 \tag{3}$$

where M is the Mach number. When the computational domain is restricted to the plasma edge, boundary conditions are also required to model the interaction with the core. In this case the dimensionless boundary conditions on the inner boundary are both of the Dirichlet type, with $n = 1$ and $\Gamma = 0$. To conclude this section, let us remark that this reduced model contains two of the key numerical issues of more complete fluid edge models, that is, taking account of the magnetic geometry complexity whilst appropriately describing the wall with the adequate Bohm boundary conditions.

3 HDG and spatial adaptivity

3.1 Hybrid Discontinuous Galerkin

In order to solve the 2D model presented we use a specific high-order solver, SOLEDGE3X-HDG, where the parallel flux is described as a compressible isothermal gas flow, while transport processes in the perpendicular plane, dominated by turbulence, are modelled as an effective diffusion[4]. It is noteworthy that the greater cost of Discontinuous Galerkin methods comes from the fact that the residuals inside one element depend on the states of neighbouring elements. This can be explained by the coupling between the degrees of freedom used to approximate an element-wise discontinuous high-order polynomial solution that increases the memory requirements for the solver. The hybridization of DG [5] modifies its discretization in order to reduce its calculation and memory cost for a given mesh while exploiting its high-order accuracy. It is possible to reduce the number of globally coupled degrees of freedom (DOF) by decoupling element solution approximations from each other, while the elemental DOFs are linked to the new face DOFs through fluxes such as in the finite volume methods. Then we can define an approximation of the solution, called the trace solution, which is defined on the element borders. Thus, using a static condensation procedure the only globally coupled DOFs are the face unknowns (trace solution). Then, it is straightforward to see the gain in term of computational time and memory, due to the fact that the number of face unknowns scales as p^{dim-1} compared to the p^{dim} scaling for elements. Going towards a more precise explanation of the HDG scheme used, we can resume it in a two-step evaluation: the finite element discretization to solve a local problem in each element, that is a weak formulation of the main system written in conservative form. Setting up the global problem is the following part of the HDG process. It lets us to solve the trace solution for the conservative variables in the entire mesh. Imposing

the continuity of the fluxes in the weak form, we derive the global problem across the element borders. Once we obtain the trace solution, it is possible to recover the elemental one in each element as a local post-process. The time discretization is fully implicit and is performed using either a first-order Backward Euler scheme or a second-order Gear scheme [4]. The non-linear terms are linearized using a classic NewtonâĂŞRaphson method.

3.2 Spatial adaptivity

When the solutions of the problem are smooth, high-order discretization methods become generally advantageous. On the other side, one of the main difficulties resides in shocks and other singular features such as large local gradients, where the approximation with high-order polynomials lose his efficiency. These features are usually found between edge and SOL around the separatrix. More useful, for facing such characteristics, is spatial adaptivity based on h-refinement, in which the mesh size is optimized by refining, locally in space and dynamically in time, the regions with stiff gradients while keeping a coarse mesh in flow regions where the solution is smooth. The main task consists in properly balancing the high-order feature (p-refinement) and the h-refinement, which is currently the area with largest commitment to achieve the goal of highest precision with the minimum cost[5]. In the ITER size simulations panorama, turbulent and strongly anisotropic edge plasmas are good candidates to evaluate the efficiency of mesh adaptivity.

3.3 How to refine

The refinement strategy used here relies on the generation of a sequence of meshes in order to iteratively reach the desired values of a quality indicator. In order to perform the meshing part, we have chosen an open-source software called Mmg [2, 3]. This library allows to implement an adaptation algorithm in which the mesh is modified according to a prescribed element size map that is created by setting the wanted edge sizes on each vertex of an existing mesh. The question then is how to set the mesh size. In the HDG code, a polynomial approximation of order p is used, and one then expects the error to scale with mesh size h as h^{p+1} for sufficiently smooth solutions. This property can then be exploited in the following manner: knowing the element mesh sizes $\{\tilde{h}_j^{(n)}\}$ and having an estimate of the elemental errors $\{\tilde{\varepsilon}_j^{(n)}\}$ on element j at iteration n of the refinement process, one can use a Richardson extrapolation [7] to give a guess of the desired mesh size at the next iteration, using the formula:

$$h_{target,j}^{(n+1)} = \exp\left(\frac{\ln(\varepsilon_{target}) - \ln(\varepsilon_j^{(n)})}{p+1} + \ln(h_j^{(n)})\right) \tag{4}$$

In the expression above, $\varepsilon_j^{(n)}$ is the nodal error obtain from the calculations and $h_j^{(n)}$ is the element size map. These two variables, are calculated in the vertices of the whole mesh [8] using the elemental areas $\{|\Omega_k|\}$ as follows:

$$h_j = \frac{\sum_{i \in S_j} |\Omega_i| \tilde{h}_i}{\sum_{i \in S_j} |\Omega_i|} \quad ; \quad \varepsilon_j = \frac{\sum_{i \in S_j} |\Omega_i| \tilde{\varepsilon}_i}{\sum_{i \in S_j} |\Omega_i|} \tag{5}$$

in which S_j denotes the set of indices of elements having node j as a vertex.

The hypothesis is that ε_{target} is local, or rather elemental, and evolves like the global error. Thus, we expect that the distribution of the error over the whole mesh, which locally depends strongly on the size of each element, can be made uniform by appropriate refinements. With this process we can decrease or increase the mesh size at the same time, both realized locally and isotropically. Indeed, in the whole procedure we can exploit both refinement and coarsening where the error is larger or lower than expected, respectively. In principle, the algorithm thus described can reach the desired accuracy in one iteration. In practice however, setting the element size at the next iteration as $h_j^{(n+1)} = h_{target,j}^{(n+1)}$ can lead to an unsatisfactory convergence of the algorithm, and it can be improved by using an alternative definition of the desired element size:

$$h_j^{(n+1)} = \sqrt{h_{target,j}^{(n+1)} \cdot h_j^{(n)}} \tag{6}$$

The latter formula dampens the adaptation process and leads to smoother convergence in our experience.

3.4 Error estimators

Output-based error estimators computed from solutions provide information on its accuracy and at the same time can drive the mesh adaptation process in the HDG discretization. The elemental error is estimated with the difference between two different solutions f of the code obtained with two consecutive orders p and $p+1$, exploiting the property of HDG method to obtain higher accuracy with very efficient computations at higher orders:

$$\varepsilon_f = \| f_{p+1} - f_p \|_{L^2} \tag{7}$$

Then we have set three different error estimator parameters to insert into the expression of a simple L^2 norm weighted by the area of the respective elements j and used to control and direct the adaptive procedure:

$$\tilde{\varepsilon}_{f,j} = \frac{1}{|\Omega_j|} \cdot \|\varepsilon_f\|_{L^2(\Omega_j)} = \frac{1}{|\Omega_j|} \left[\int_{\Omega_j} (f_{p+1} - f_p)^2 \, d\Omega \right]^{1/2} \tag{8}$$

where f is chosen between the density n, the flux Γ and the mach number M. The control parameter used to stop the adaptive iteration process is the

global error, calculated with the contributions from all the elements N_e in the domain:

$$\varepsilon_{glob} = \sqrt{\sum_{i=1}^{N_e} \|\varepsilon_f\|^2_{L^2(\Omega_j)}} \tag{9}$$

where f represents one the parameters chosen as said. The entire process is set in this way: first, we set the target precision for the global error. Then, we let the code going to convergence with the Newton-Raphson iterations for the initial mesh. At this point it is needed a stopping criterion, so we compare the global error obtained with the target set and if it is not included in a 10% range, the adaptive part starts. Thus, we create a new mesh using the element size map based on the h_j^{n+1} which in turn is based on a specific estimator as mentioned above. Eventually, the calculation with the HDG code is repeated on the new mesh and this process is performed iteratively until the stopping condition is satisfied.

4 Results

In the present work, all computations presented have been performed with the polynomial order $p = 5$, which provides the best trade-off between accuracy and computing time. The results shown below refer to the geometry of the tokamak WEST. After the evaluations of the three error estimators, we came to the conclusion that the density-based one is the most reliable and shows the most encouraging results compared with the the estimator based on particle flux Γ or Mach number. Figure 1shows four consecutive stages

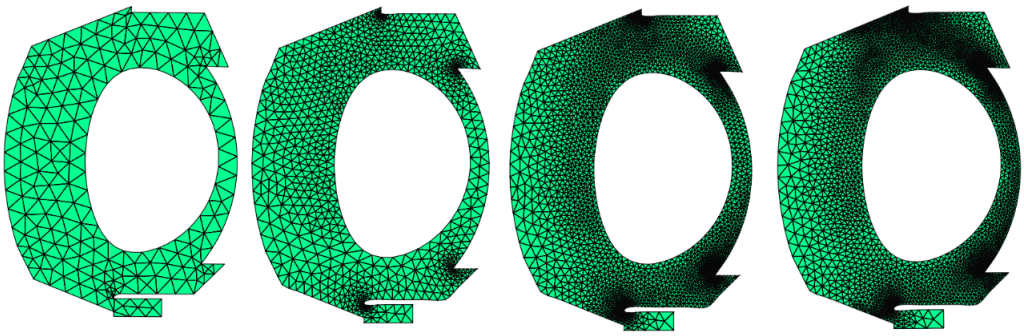

Figure 1: Sequence of consecutive refinements and coarsening (from left to right) starting with a initial coarse mesh of uniform size. The error estimator used to drive the process is based on the density n with the target error set at 10^{-4}.

of the refinement process outlined above. It indeed shows a non-uniform refinement, which highlights specifically known sources of error which are

the mesh singularities induced by the wall geometry and especially limiters. These singularities are demanding as they often correspond to regions where the Mach number switches sign across the magnetic surface crossing the corner as a result of the Bohm boundary conditions. The solution obtained from the last mesh, where the convergence of the adaptive process based on a target of precision of the global error set at 10^{-4} is reached, is shown in Figure 2(top). One questionable aspect of the final mesh is that the resolution is relatively fine in the core compared to the SOL, although both density and Mach number seem smooth in this region. This aspect is likely related to the fact that density has larger values in the core. Another aspect worth noticing comes from Figure 2 (bottom), where is evident how the evaluation of the error globally becomes more uniform going through the various iterations in respect with the global target precision (10^{-4}) demanded from the beginning.

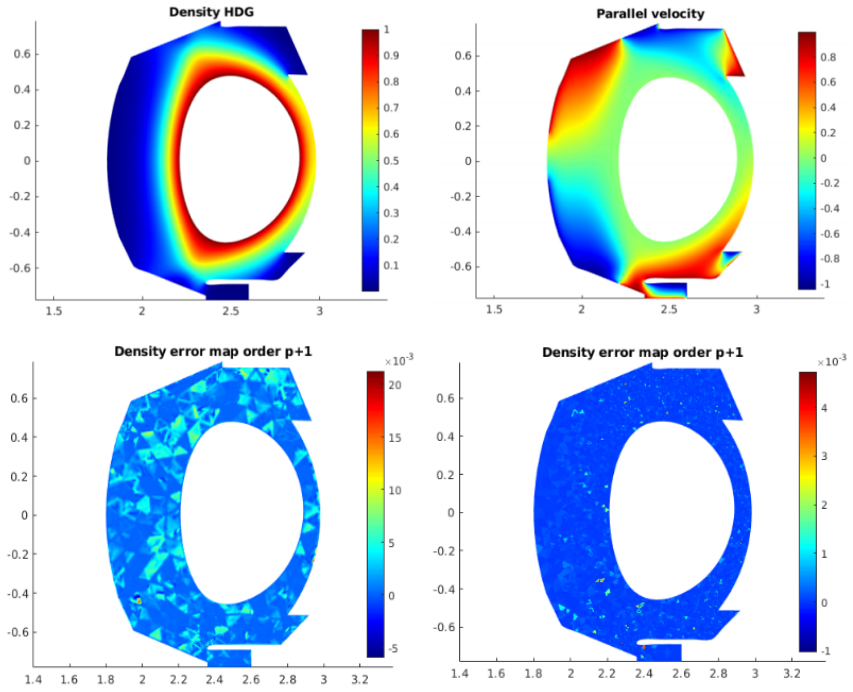

Figure 2: Top: solution for the density and parallel velocity at the last iteration of the adaptive process. Bottom: error map plots at the first and last iteration. The error estimator used to drive the process is based on the density n and it is projected on the higher order $p + 1 = 6$.

This last aspect notwithstanding, an interesting remark can be made on the calculation time shown in Table 1. This Table shows estimated errors resulting from computations with uniform meshes, as well as estimated errors computed with adaptive refinement. It illustrates an evident gain in terms of

number of DOFs using the adaptive process: the adaptive refinement requires at least twice fewer DOFs to reach the target precision 10^{-4}, a precision that even the most refined uniform mesh could not reach. It is worth noting that the solution with the uniform mesh does not converge at the theoretically expected rate for a $p = 5$ approximation, likely as a consequence that the exact solution seems not to be arbitrarily smooth around corners in the wall geometry. The adaptive results generally require fewer DOFs, as they show strong refinement around the location of these supposed discontinuities in order to provide a uniform decrease of error over the whole computational domain, as illustrated in Figure 2 (bottom). Thus, they achieve a much faster accuracy enhancement as shown between iterations 3 and 4 of the refinement, where a 3-fold decrease of the estimated error is observed whilst the number of elements is increased by a mere 23%. In the whole process the cost of the adaptive part is negligible in respect with code calculations. Finally, one can remark that the user input is limited: an initial mesh must be provided, which will then be automatically adapted in order to reach the estimated error level requested.

Table of results for $p = 5$ adaptive				Table of results for $p = 5$ non adaptive			
Iteration	ε_{glob}	$nDOF$	N_e	h	ε_{glob}	$nDOF$	N_e
1	$4.43{\cdot}10^{-3}$	8148	388	0.1	$4.44 \cdot 10^{-3}$	8148	388
2	$5.46{\cdot}10^{-3}$	35133	1673	0.09	$5.72 \cdot 10^{-4}$	21819	1039
3	$2.99{\cdot}10^{-4}$	109263	5203	0.02	$2.49 \cdot 10^{-4}$	307692	14652
4	$1.07{\cdot}10^{-4}$	134757	6417				

Table 1: Left: results for the polynomial order $p = 5$ for 4 refinement iterations, showing the global error ε_{glob}, the number of degrees of freedom and the number of element referring to the adaptive sequence of meshes towards the convergence. Right: results for the polynomial order $p = 5$ three different uniform meshes with decreasing mesh size.

5 Conclusions

This paper presents an adaptive mesh refinement for a reduced 2D model for ion density n and particle flux Γ in the direction parallel to the magnetic field. The strategy draws on the ease provided by HDG discretization to provide local error estimates using order p and $p + 1$ computations on the same mesh, which are then fed back into mesh generation library which allows to design the mesh through the use of an element size map. The map size is constructed by combining the error estimate with a Richardson extrapolation that provides a guess for the local mesh size required for the desired error level. This strategy has been shown to converge to required

estimated error, whilst providing a significant improvement on the number of DOFs to reach the target when compared to uniform mesh. This strategy takes only simple inputs from the user, automatically adapting the mesh in areas where it is needed. The results shown are preliminary, as they do not cover a more complex edge model. The strategy has therefore to be tested in more demanding situations, but it provides the basis of a user-friendly manner of simulating plasma edge transport.

6 Acknowledgements

This work has been carried out within the framework of the EUROfusion Consortium and has received funding from the Euratom research and training programme 2014-2018 and 2019-2020 under grant agreement No 633053. The views and opinions expressed herein do not necessarily reïňĆect those of the European Commission. This work has been also supported by the French National Research Agency grant SISTEM (ANR-19-CE46-0005-03).

References

[1] G. Giorgiani et al, An hybrid discontinuous galerkin method for tokamak edge plasma simulations in global realistic geometry, J. Comp. Phys. (2018)

[2] C.Dobrzynski, P.Frey, Anisotropic Delaunay mesh adaptation for unsteady simulations, 2008, Proceedings of the 17th international Meshing Roundtable

[3] C. Dapogny, C. Dobrzynski and P. Frey, Three-dimensional adaptive domain remeshing, implicit domain meshing, and applications to free and moving boundary problems, April 1, 2014, JCP, 262, pp. 358âĂŞ378

[4] Giorgiani G, Camminady T, Bufferand H, Ciraolo G, Ghendrih P, Guillard H, Heumann H, Nkonga B, Schwander F, Serre E and Tamain P. A new high-order fluid solver for tokamak edge plasma transport simulations based on a magnetic-field independent discretization, Contributions to Plasma Physics 2018;58:688âĂŞ695.

[5] K. J. Fidkowski: Comparison of hybrid and standard discontinuous Galerkin methods in a mesh-optimisation setting, International Journal of Computational Fluid Dynamics (2019)

[6] L. Demkowicz, Computing with HP-adaptive Finite Elements - One and Two Dimensional Elliptic and Maxwell Problems, Volume 1. (2006)

[7] L.F. Richardson, The approximate arithmetical solution by finite differences of physical problems including differential equations, with an application to the stresses in a masonry dam. (1911) Philosophical Transactions of the Royal Society A. 210 (459âĂŞ470): 307âĂŞ357.

[8] Patrick M. Knupp, Algebraic mesh quality metrics for unstructured initial meshes, Finite Elements in Analysis and Design 39 (2003) 217 âĂŞ 241